
Article:
Ding, F., Fu, L., Huang, X. et al. (3 more authors) (2025) Self-healing carboxymethyl chitosan hydrogel with anthocyanin for monitoring the spoilage of flesh foods. Food Hydrocolloids, 165. 111270. ISSN 0268-005X

https://doi.org/10.1016/j.foodhyd.2025.111270

Food Hydrocolloids

Self-healing carboxymethyl chitosan hydrogel with anthocyanin for monitoring the spoilage of flesh foods

--Manuscript Draft--

Manuscript Number:	FOODHYD-D-24-04020
Article Type:	Research paper
Keywords:	Smart packaging; Carboxymethyl chitosan; Hydrogel; Anthocyanin; Biodegradability
Corresponding Author:	Fuyuan Ding Jiangsu University Zhenjiang, China
First Author:	Fuyuan Ding
Order of Authors:	Fuyuan Ding
	Lin Fu
	Xiaowei Huang
	Jiyong Shi
	Megan Povey
	Xiaobo Zou
Abstract:	Self-healing hydrogels prepared with biopolymers have been widely applied in various engineering fields. In this study, carboxymethyl chitosan (CMC) hydrogels have been prepared and applied in smart food packaging fields. The carboxymethyl chitosan hydrogels were fabricated through crosslinking method with oxidized alginate (ADA). The concentration of oxidized alginate has greatest impact on the physicochemical properties of the hydrogels. Due to the dynamic properties of Schiff base linkages and hydrogen bonds, the hydrogel demonstrated self-healing and 3D printing properties. Higher concentrations of oxidized alginate result in weaker self-healing ability of the hydrogels. The anthocyanin (An) in the hydrogel exhibited a color change when exposed to acidic and basic gases, making the hydrogel potentially useful for smart indicators. These intelligent indicators can be used to detect the freshness of chicken, pork and fish. In addition, the hydrogel showed excellent biodegradable properties and can be degraded in lake, soil and simulated seawater. The self-healing, biodegradable and pH sensitive hydrogels has the potential to be applied in smart food packaging.
Suggested Reviewers:	Ubonratana Siripatrawan Chulalongkorn University Ubonratana.S@chula.ac.th
	Lingyun Chen University of Alberta lingyun.chen@ualberta.ca
	Yixiang Wang Universite McGill yixiang.wang@mcgill.ca
	Juan Du Singapore Institute of Technology du.juan@singaporetech.edu.sg

Dear Editor

I am writing to submit our manuscript entitled " Self-healing carboxymethyl chitosan hydrogel with anthocyanin for monitoring the spoilage of flesh foods" for consideration as a Research Article in Food Hydrocolloids.

In this work, we developed novel carboxymethyl chitosan (CMC) hydrogels crosslinked with oxidized alginate (ADA), designed for application in smart food packaging. The hydrogels exhibit self-healing properties, excellent biodegradability and 3D printable properties. The anthocyanin (An) in the hydrogel provides a visual indication of food freshness through color changes when exposed to acidic or basic gases. This pH-responsive behavior makes the hydrogel particularly suitable for intelligent packaging. The hydrogels can be used as smart indicators to monitor the freshness of perishable food items such as chicken, pork, and fish. In addition, the hydrogels were found to degrade effectively in natural environments such as lake water, soil, and simulated seawater, making them environmentally friendly alternatives in packaging technology.

We believe that our findings will contribute to the growing field of sustainable food packaging solutions. Thank you for your time and consideration. We look forward to your feedback.

Sincerely yours
Fuyuan Ding

Highlights

- CMC hydrogels showed self-healing and 3D-printable properties
- pH-sensitive hydrogels can be used to detect freshness of flesh foods
- Hydrogels are biodegradable in lake water, soil, and simulated seawater
- Oxidized alginate concentration affects hydrogels' physicochemical traits

Graphical Abstract

TOC Figure

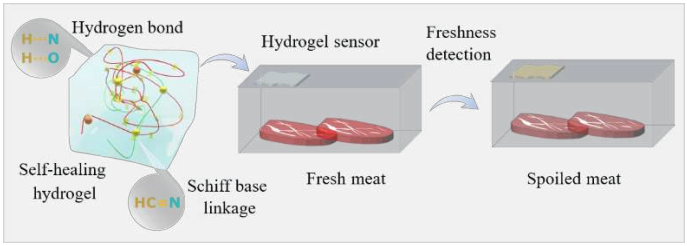

Self-healing carboxymethyl chitosan hydrogel with anthocyanin for monitoring the spoilage of flesh foods

Fuyuan Ding*[,a], Lin Fu[a], Xiaowei Huang[a], Jiyong Shi[a], Megan Povey*[,b], Xiaobo Zou*[,a]

[a]International Joint Research Laboratory of Intelligent Agriculture and Agri-products Processing, Joint Laboratory of China-UK on Food Nondestructive Sensing, School of Food and Biological Engineering, Jiangsu University, Zhenjiang, 212013, China

[b]School of Food Science and Nutrition, University of Leeds, Leeds LS2 9JT, UK

*Corresponding author:

Email: dingfuyuan@ujs.edu.cn; (F. Ding)

Email: M.J.W.Povey@food.leeds.ac.uk; (M. Povey)

Email: Zou_xiaobo@ujs.edu.cn; (X. Zou)

Abstract

Self-healing hydrogels prepared with biopolymers have been widely applied in various engineering fields. In this study, carboxymethyl chitosan (CMC) hydrogels have been prepared and applied in smart food packaging fields. The carboxymethyl chitosan hydrogels were fabricated through crosslinking method with oxidized alginate (ADA). The concentration of oxidized alginate has greatest impact on the physicochemical properties of the hydrogels. Due to the dynamic properties of Schiff base linkages and hydrogen bonds, the hydrogel demonstrated self-healing and

3D printing properties. Higher concentrations of oxidized alginate result in weaker self-healing ability of the hydrogels. The anthocyanin (An) in the hydrogel exhibited a color change when exposed to acidic and basic gases, making the hydrogel potentially useful for smart indicators. These intelligent indicators can be used to detect the freshness of chicken, pork and fish. In addition, the hydrogel showed excellent biodegradable properties and can be degraded in lake, soil and simulated seawater. The self-healing, biodegradable and pH sensitive hydrogels has the potential to be applied in smart food packaging.

Keywords: Smart packaging; Carboxymethyl chitosan; Hydrogel; Anthocyanin; Biodegradability

1. Introduction

Hydrogels are three-dimensional (3D) structures comprising a crosslinked polymeric network which have been widely used in tissue engineering, environmental and drug delivery fields due to the high-water content, soft nature, and high porosity of this material (Chirani, Yahia, Gritsch, Motta, Chirani, & Farè, 2015). Specifically, those biopolymer derived hydrogels with excellent biocompatibility and biodegradability showed great potential in different engineered fields (Muir & Burdick, 2020; Patel & Thareja, 2022). Chitosan is a widely used biopolymer which can be fabricated into different kinds of hydrogels (Ding, Nie, Deng, Xiao, Du, & Shi, 2013; Yan, Ding, Bentley, Deng, Du, Payne, et al., 2013). Carboxymethyl chitosan is one of the most important derivatives of chitosan (Ding, Hu, Lan, & Wang, 2020). Carboxymethyl chitosan hydrogel can be prepared through chemical or physical methods (Upadhyaya, Singh, Agarwal, & Tewari, 2013). For instance, carboxymethyl chitosan hydrogel fabricated through chelation showed excellent

antibacterial properties and high toughness and has the potential to be applied in food packaging (Z. Lin, Bi, Du, Zhang, Fu, Fu, et al., 2023). Carboxymethyl chitosan hydrogel crosslinked by Schiff base linkage showed excellent self-healing properties and can be applied in various fields (Lou, Tian, Deng, Wang, & Jiang, 2020; Yin, Song, Chen, Huang, & Huang, 2022).

Self-healing polymeric hydrogels are an innovative type of material developed in the last two decades (Ding, Li, Du, & Shi, 2018) and have been widely used in the fields of tissue engineering and drug delivery (Guadagno, Vertuccio, Barra, Naddeo, Sorrentino, Lavorgna, et al., 2021). Their self-healing properties endow them with 3D printing properties which expand their application (Gopalakrishnan & Mishra, 2023). However, self-healing polymeric materials have rarely been applied as food packaging materials (K. Huang & Wang, 2022; Lai, 2023) despite their ability to extend the functionality of packaging and maintain its integrity (Ding, Wu, Wang, Xiong, Li, Li, et al., 2015). Coatings made from chitosan and alginate showed self-healing properties and can be used as anti-fog packaging (Hu, Chen, Lan, Ren, Wu, Liu, et al., 2018). Multilayer films prepared with chitosan and carboxymethyl cellulose showed self-healing properties and can be used to extend the shelf-life of lemon (Sultan, Hafez, & Saleh, 2022). Multifunctional waterborne polyurethane films with self-healing properties can be used as smart packaging to monitor the freshness of shrimp (Sai, Zhang, Qu, Wang, Zhu, Bai, et al., 2022). Such self-healing polymeric materials showed great promise in food packaging.

Here, we prepared a hydrogel with carboxymethyl chitosan (CMC), oxidized alginate (ADA) and anthocyanin (Scheme 1). The amino groups in carboxymethyl chitosan can be crosslinked with aldehyde groups in the oxidized alginate through a Schiff base linkage (Shen, Wang, Wang, Meng, & Zhao, 2021; Yin, Song, Chen, Huang, & Huang, 2022). The anthocyanin can be attached to the

carboxymethyl chitosan and oxidized alginate chains via electrostatic interaction and hydrogen bonds (Cao, Wang, Wang, Lin, Niu, Guo, et al., 2023; F. Wang, Xie, Tang, Hao, Wu, Sun, et al., 2023). Dynamic hydrogen bonds and Schiff base linkages confer self-healing properties to the hydrogel without any stimulus (Gopalakrishnan & Mishra, 2023; Shen, Wang, Wang, Meng, & Zhao, 2021). The anthocyanin in the hydrogel showed pH sensitive properties which endows them with potential application in smart packaging fields (X. Zhang, Chen, Dai, Cui, & Lin, 2024). The creativity and significance of the present work on hydrogels are as follows: (1) Methods of preparation are mild and toxic solvent free which is critical for the hydrogels to be applied in food packaging field. (2) They show excellent self-healing properties which can be potentially applied as bio-ink in 3D food printing. (3) They show rapid color response to the acidic and basic gases which endow the hydrogels with the ability to detect the freshness of different meats. Self-healing carboxymethyl chitosan hydrogel with biodegradability and color response to different pHs can potentially be applied in smart packaging.

Scheme 1

2. Material and methods

2.1 Materials

Carboxymethyl chitosan (CMC) was purchased from Macklin Co., Ltd. (Shanghai, China). The molecular weight is 120 kDa. The degree of carboxymethyl group in the modified chitosan is 0.8 tested by titration. Sodium alginate, sodium periodate, ethylene glycol, ethanol, acetic acid, ammonium hydroxide, phosphate buffer saline (PBS), dibasic sodium phosphate and sodium dihydrogen phosphate were bought from China National Pharmaceutical Group Corp. Purple sweet

potato, salmon, chicken and pork were purchased from a local grocery store (Zhenjiang, China). Deionized water was used in all experiments.

2.2 Preparation of oxidized alginate

The oxidized alginate (ADA) with an oxidation degree about 50% was prepared according to our previous reported method (Ding, Dong, Wu, Fu, Tang, Zhang, et al., 2022). Briefly, 10 g sodium alginate and 5.4 g sodium periodate were mixed with 300 mL water and then stirred at 25℃ in the dark. After 5 hours, 3.5 mL ethylene glycol was added and stirred for another 0.5 hours to remove unreacted sodium periodate. After that, the solution was mixed with 300 mL ethanol and white precipitate was obtained through filtration. Finally, the filtrate was lyophilized under vacuum and the oxidized sodium alginate was obtained. The degree of oxidation was obtained according to the reported method and was about 47%.

2.3 Extraction of anthocyanin

Purple sweet potato was washed and peeled and then dried at 60 ℃. The potato was made into powder by grinding. The powder (50.0 g) was then mixed with 50% ethanol (500 mL) and the mixture was placed in a thermostatic water bath at 60℃ for 3 hours. After 3 hours, the ethanol was removed in a rotary evaporator (RE-200B, Shang Hai Yarong Biotechnology, China) to obtain anthocyanin concentrate which was then lyophilized under vacuum to obtain anthocyanin extract.

We determined the anthocyanin content by the extinction coefficient method. 1 mL anthocyanin concentrate was firstly mixed with 10 mL buffer solution (pH 1.0 and pH 4.5), and then the mixture was put into a quartz cuvette. Next, the absorbance of the mixture was measured at 525

nm and 700 nm. The content of anthocyanin was calculated by the following formula:

$$W\,(\mathrm{mg/L}) = A \cdot DF \cdot M \times 103/(\varepsilon \cdot L)$$

Where W is the content of anthocyanin, A is the absorbance, $A = (A_{525nm}\text{-}A_{700nm})_{pH1.0} - (A_{525nm}\text{-}A_{700nm})_{pH4.5}$, DF is the dilution factor (10), M is the molecular weight of cyanidin-3-o-glucoside (484.84 g/mol), ε is the extinction coefficient of cyanidin-3-o-glucoside (26900), L is the optical path (1 cm). After analysis, the anthocyanin content was 123.38 mg/L.

2.4 Preparation of the composite hydrogels

Carboxymethyl chitosan solution with a concentraiton of 7 wt% was prepared in deionized water. The oxidized alginate solution with a concentration of 5.0 wt% was also prepared in deionized water. Then, the CMC solution contained anthocyanin (0.75 wt%) was mixed with ADA solution according to the dry weight of CMC vs ADA as 1:0.1, 1:0.2, 1:0.3 and the hydrogel was coded as hydrogel-1, hydrogel-2, hydrogel-3. In addition, the hydrogel with different amount of anthocyanin (0.0 wt%, 0.75 wt%, 1.50 wt%, 2.25 wt% against the dry weight of CMC) was prepared and coded as hydrogel-4, hydrogel-2, hydrogel-5, hydrogel-6.

2.5 Characterization of the hydrogel

The formation of the hydrogel was investigated by the bottle inversion method. The mixture of CMC, ADA and dye was prepared and placed in a glass bottle. After 20 min, the glass bottle was inverted. The state of the hydrogel in the glass bottle was observed and recorded by a digital camera.

Fourier-transform infrared spectroscopy (FT-IR) spectra of CMCS, ADA, anthocyanin and gel were recorded on an infrared spectrometer (Nicolet iS50, Thermo Nicolet Inc., USA) by the KBr

method from 400 to 4000 cm^{-1} at several scans of 32 and a resolution of 4 cm^{-1}.

The thermal properties of hydrogels were carried out by using a thermal gravimetric analyzer (TA, TGA 550, USA). 5 mg lyophilized hydrogel was put into a sealed aluminum pot and heated from 0°C to 800°C at the rate of 10 °C/min in the nitrogen gas environment.

X-ray diffraction (XRD) spectra of CMCS, ADA, anthocyanin and lyophilized hydrogel were analyzed by an X-Ray diffractometer (D8 ADVANCE Bruker, Germany) furnished with a Cu Ka radiation source (λ = 1.5406 Å) with an angular range of 5° to 90° with steps of 5° (2 θ)/min。

A scanning electron microscope (SEM) (Ultra, Carl Zeiss AG, Germany) was used to observe the surface and cross-section of hydrogel at an accelerating voltage of 7 kV. Before test, the hydrogel was lyophilized for 2 days. Then, the dried gel was cut, and the samples were coated with gold.

Rheological characteristics of hydrogel (height of 1 mm) was analyzed by a rheometer (RS6000, Malvern Instruments) with a 40 mm flat plate, at 25 °C, a frequency of 1 Hz, and a strain of 1%. Silicone oil was applied to avoid solution volatilization.

Mechanical characteristics of hydrogel (length of 40 mm and width of 10 mm) were analyzed using a TA.XT2i (Stable Microsystems) texture analyzer. The strain rate was set to 2 mm/s. The breaking elongation of hydrogel and tensile strength of hydrogel were calculated using the following formula.

$$\delta\ (\%) = (L_1/L_0) \times 100\ \%$$

$$R_m\ (\text{mPa}) = F/(w \cdot h)$$

Where δ is elongation at break of hydrogel; L_1 is breaking length (mm); L_0 is original length (mm); R_m is tensile strength; F is maximum tensile force (N); w is width (mm) and h is thickness (mm).

155 **2.6 Self-healing properties of the hydrogel**

156 The hydrogel was formed in a cylindrical container. The prepared hydrogel was cut from the
157 middle and then put back into the container so that the two cutting surfaces were contact closely.
158 After 2 hours, the hydrogel was stretched by two tweezers, and self-healing of the hydrogels was
159 recorded by a digital camera.

160 A rheological test to characterize the self-healing properties of hydrogel was performed on a
161 rheometer (RS6000, Malvern Instruments) with a 40 mm flat plate. The temperature was set to 25 ℃,
162 the frequency was 1 Hz, and the strain was 1%. Silicone oil was applied to avoid volatilization of
163 the solution.

164

165 **2.7 Analysis of swelling behavior**

166 The hydrogel was placed in buffer solution (pH 3.0, pH 7.4 and pH 9.5). The weight change of
167 the hydrogel was measured at designed time intervals. After the swelling of hydrogel reached
168 equilibrium, the measurement was stopped. The swelling rate was calculated using the following
169 formula.

170 $SR\ (\%) = (M_t - M_0)/M_0 \times 100$

171 Where SR is equilibrium swelling rate; M_t is weight at designed time intervals and M_0 is the original
172 weight.

173

174 **2.8 pH response of the hydrogels**

175 The color change of the hydrogels was measured with a color meter (Konica Minolta CM-
176 2600). The hydrogel (2 cm×2 cm) was exposed to acetic acid and ammonia gas respectively for 2

minutes, and lightness (L), red-green value (a), yellow-blue (b), and the total color difference (ΔE) were recorded. The circular response to the acetic acid and ammonia gas was also conducted. The hydrogel was exposed to acetic acid or ammonia gas alternately for 2 minutes, and CIELab ΔE change was measured.

2.9 Fresh meat spoilage trial

50 g of grass carp, pork and chicken with uniform appearance were put into boxes at 15°C. The hydrogels were used as smart indicators and placed on the top of the box. The color change of the label was recorded by a digital camera and the color parameters were obtained through a color meter. The pH change of the meat was recorded through a pH meter (Testo 205). The TVB-N of the meat was obtained on an automatic Kjeldahl nitrogen analyzer (Hanon, K1100F, China).

2.10 3D printing properties

The CMCS, ADA and anthocyanin solutions were mixed evenly, and then, the mixture was placed in a syringe tube (the needle diameter is 100 μm) installed on the 3D food printer with a moving speed of 0.5 mm s^{-1}, and extrusion pressure of 0.3 MPa. Different gel ratios and different substrates (paper and bread) were used for printing. The printing effect was observed and recorded by a digital camera.

2.11 Biodegradability of the hydrogel

The hydrogel was placed in soil, lakes and stimulated sea water to study the biodegradable properties. As to the degradation in the soil, the hydrogel was placed in a nylon fabric (500 mesh)

and buried 20 cm under the soil. The degradation of the hydrogel in lakes was conducted in Jiangsu University campus. The degradation of hydrogel in sea water was conducted in a stimulated sea water with a NaCl concentration of 3.5‰. The weight change of the hydrogel was recorded at designed time intervals and the appearance of the hydrogel was recorded using a digital camera.

3. Results and discussion

3.1 Preparation of the hydrogel

Schiff base linkage is a dynamic bond that has been widely applied to prepare biopolymeric hydrogels (Xu, Liu, & Hsu, 2019; Zhou, Chen, Guan, & Zhang, 2014). Here, we mixed two biopolymers to prepare a hydrogel through Schiff base linkage. Fig. 1 (A) shows the schematic and digital images of the formation of hydrogels through mixing the two biopolymers. The amino groups in CMC can be crosslinked by aldehyde groups in ADA to form hydrogels (Ma, Su, Ran, Ma, Yi, Chen, et al., 2020; Zhao, Feng, Lyu, Yang, Lin, Bai, et al., 2023). The anthocyanin can be attached to the hydrogel by electrostatic interaction and hydrogen bonding. As shown in Fig. 1 (A), the content of ADA in the mixture has a large influence on the gel formation properties. When the CMC *vs* ADA was set as 1:0.1, a weak hydrogel can be prepared. Further increasing the content of ADA, the gel strength was improved. The hydrogel remained static on the top of an inverted bottle when the ratio of CMC *vs* ADA increased to 1:0.2 and 1:0.3. This was attributed to increased Schiff base linkage formed when content of ADA in the mixture increased (Ding, Shi, Wu, Liu, Deng, Du, et al., 2017).

The formation of the hydrogel was firstly investigated by the FT-IR technology. As shown in Fig. 1 (B), FT-IR spectra of CMC, ADA, anthocyanin, hydrogel-2 and hydrogel-4 were obtained to

221 characterize the interaction of biopolymers and the dye. In the spectrum of CMC, the peak around
222 3425 cm^{-1} was assigned to the free stretching vibration of intermolecular and intramolecular O−H.
223 The two characteristic bands at 2936 cm^{-1} and 2864 cm^{-1} were attributed to the stretching vibration
224 and bending vibration of $C-H_2$ and C−H. The peak at 1623 cm^{-1} was the characteristic peak of
225 carboxyl group which corresponded to the anti-symmetrical stretching vibration absorption peak
226 (COO) (Virk, Virk, Liang, Sun, Zhong, Tufail, et al., 2024). The symmetrical stretching vibration
227 absorption peak of carboxyl group was located at 1426 cm^{-1}. The peak at 1062 cm^{-1} corresponded
228 to the C–OH stretching vibration absorption peak in carboxymethyl chitosan (Ding, Hu, Lan, &
229 Wang, 2020). After adding oxidized alginate and anthocyanin to prepare hydrogel, some changes
230 occurred in the FT-IR spectrum of hydrogel-4 and hydrogel-2. In the FT-IR spectrum of hydrogel-
231 4, the peak at 2936 cm^{-1} became sharp and the peak at 1623 cm^{-1} shifted to 1600 cm^{-1} which
232 indicated that the oxidized alginate had been successfully crosslinked with carboxymethyl chitosan.
233 The peak shift from 1623 cm^{-1} to 1600 cm^{-1} may be due to the formation of Schiff base linkage
234 between two biopolymers (Cui, Cheng, Li, Khin, & Lin, 2023; Ding, et al., 2015). The peak around
235 3425 cm^{-1} broadens which indicated that hydrogen bonds had formed between CMC and ADA
236 (Ding, et al., 2022). After adding anthocyanin to the hydrogel, the peak around 3425 cm^{-1} broadened
237 due to hydrogen bond formation between the two polymers and dye. Other peaks in the FT-IR
238 spectrum of hydrogel-2 showed no significant changes compared with the hydrogel-4 which may
239 be due to the low content of anthocyanin.

240 The hydrogel was further characterized by the X-ray diffraction technology. As shown in Fig.
241 1 (C), the strong peak at $2\theta = 20°$ was the characteristic peak of CMC. The peak at around $2\theta = 23°$
242 was the characteristic peak of oxidized alginate. In the XRD spectrum of hydrogel-4, there appeared

243 a strong peak at around 2θ = 23° which demonstrated that the oxidized alginate had crosslinked with
244 carboxymethyl chitosan to from hydrogel. The peak at around 2θ = 23° weakened after adding
245 anthocyanin. This may be attributed to hydrogen bond and ionic interactions between oxidized
246 alginate, carboxymethyl chitosan and anthocyanin that influenced the crystal structure (Alnadari,
247 Al-Dalali, Pan, Abdin, Frimpong, Dai, et al., 2023; H.-L. Huang, Tsai, Lin, Hang, Ho, Tsai, et al.,
248 2023; Santos, Alves-Silva, & Martins, 2022).

249 The morphology of the hydrogel was studied by optical microscope and scanning electron
250 microscope. The morphologies of hydrogel-2 and hydrogel-4 were recorded. As shown in Fig. 1 (D),
251 the digital images showed that the morphologies of both hydrogel-2 and hydrogel-4 were porous
252 structures. The morphologies were further studied by scanning electron microscope. As shown in
253 Fig. 1 (D), the hydrogel-2 and hydrogel-4 showed a porous structure which indicated that the
254 incorporation of anthocyanin had little effects on the morphologies of the hydrogel.

255 The effect of oxidized alginate and anthocyanin on the thermal properties of CMC were studied.
256 Fig. 1 (E) shows the thermogravimetric (TG) curves of CMC, hydrogel-4 and hydrogel-2. The
257 reduction in weight of samples between 30℃ to 105℃ was attributed to the evaporation of adsorbed
258 water. Decomposition of CMC, hydrogel-2 and hydrogel-4 occurred between 250℃ and 500℃ with
259 a rapid weight loss of about 60% which was attributed to the thermolysis of the carbohydrate. The
260 thermogravimetric differential (DTG) curve in Fig. 1 (F) gives a decomposition temperature of
261 CMC at 285.5℃. The decomposition temperature of CMC crosslinked with oxidized alginate
262 (hydrogel-4) is 265.5℃. The decomposition temperature of hydrogel was lower than the CMC due
263 to the amorphous structure of the oxidized alginate. The hydrogel with anthocyanin (hydrogel-2)
264 has similar decomposition temperature with the hydrogel-2 without dye. This may be attributed to

the fact that the concentration of anthocyanin in the hydrogel is low and anthocyanin is an amorphous structure.

Fig. 1

3.2 Self-healing of the hydrogel

Due to the dynamic properties of the Schiff base linkage and hydrogen bonds, the hydrogel showed self-healing properties (J. Wang, Gao, Zhao, & Ju, 2023). As shown in Fig. 2 (A), the sliced two semicircle hydrogels with 0.75 wt% anthocyanin healed into an integral circle hydrogel after 1 hour. The healed hydrogel can be stretched which demonstrated excellent self-healing ability. The self-healing properties of the hydrogel were mainly derived from the reconstruction of Schiff base linkage and hydrogen bonds at the interface of the cut surface. The anthocyanin in the hydrogel has little effect on the self-healing ability. As shown in Fig. 2 (A), the hydrogel (CMC vs ADA 1:0.2) with different concentration of anthocyanin (0 wt%, 0.75 wt%, 1.5 wt%, and 2.25 wt%) can self-heal into an integral hydrogel and can be stretched after incubating for 1 hour. This was due to the low concentration of anthocyanin in the hydrogel and hydrogen bonding is weak. The Schiff base linkage in the hydrogel has a large influence on the self-healing ability of the hydrogel. As shown in Fig. 2 (A), the hydrogel with CMC vs ADA as 1:0.1 and 1:0.2 can self-heal and the healed hydrogel can be stretched. However, the hydrogel prepared with CMC vs ADA as 1:0.3 possessed poor self-healing properties. The self-healed hydrogel cannot be stretched after self-healing for 1 hour. More ADA in the hydrogel resulted in fewer free amino groups at the cut interface and a more rigid network which decreased the self-healing ability (Ding, et al., 2015).

The self-healing ability of the hydrogel was then evaluated by the rheology tests. The elastic

287 responsive properties of hydrogel-2 were recorded. Note that since the hydrogel without
288 anthocyanin (hydrogel-4) had similar self-healing ability with the hydrogel-2, the elastic response
289 of hydrogel-4 had not been recorded. As shown in Fig. 2 (C), *G*' was slightly higher than the *G*" at
290 a strain of 10% which indicated the hydrogel was a solid hydrogel state. When the strain amplitude
291 was increased to 1000% at 1.0 Hz, *G*' decreased and was lower than *G*". This indicated that the
292 hydrogel network had collapsed and turned into a sol state at high strain. Then, the hydrogel was
293 subjected to an alternatively changing amplitude of oscillatory force to investigate the elastic
294 response of the hydrogel. *G*' quickly recovered and was higher than *G*" when the strain returned to
295 10%. This was attributed to the excellent responsive properties of the hydrogel network. *G*'
296 increased in step with the number of experimental cycles. This may be due to the fast crosslinking
297 of CMC and ADA enhanced the mechanical properties of hydrogel.

298 The self-healing efficiency of the hydrogel with or without anthocyanin was obtained. Note
299 that the mechanical properties of the hydrogel prepared with CMC vs ADA as 1:0.1 was too weak
300 and self-healing ability of hydrogel with CMC vs ADA 1:0.3 is weak. The self-healing efficiency of
301 hydrogel-2 and hydrogel-4 was studied. The fracture stress of the origin hydrogel and the hydrogel
302 self-healed for 0.5 and 1 hour were recorded. As shown in Fig. 2 (D), the fracture stress of hydrogel-
303 4 was 5.7 kPa. The fracture stress of self-healed hydrogel-4 was 5.3 kPa after healing for 30 minutes.
304 The self-healing efficiency of hydrogel-4 was about 93% which demonstrated that the hydrogel
305 possessed excellent self-healing performance. The fracture stress does not increase when the healing
306 time is further increased. The hydrogel with anthocyanin (hydrogel-2) had similar self-healing
307 efficiency as hydrogel-4 which indicated that the dye had little effect on self-healing properties. The
308 phenomenon was corresponding to the self-healing properties characterized by digital images.

Fig. 2

3.3 Mechanical property of the hydrogel

The mechanical properties of the hydrogels were investigated on a TA.XT2i texture analyser. The fracture stress and elongation at break (EAB) were obtained. Hydrogel-1 is too weak to be clipped on the texture analyser and data could not be obtained. As shown in Fig. 3 (A), the fracture stress of hydrogel-4 was about 5.8 kPa when the CMC vs ADA was set to be 1:0.2. The fracture stress of the hydrogel (hydrogel-2,5,6) with different concentration of anthocyanin was close to the hydrogel-4 without dye. This was due to the low concentration of anthocyanin in the hydrogel and the interaction between anthocyanin and the polymer was weak. The mechanical properties of hydrogel were mainly influenced by the concentration of ADA in the hydrogel (Ding, et al., 2017). When the CMC vs ADA was set to be 1:0.3, the fracture stress of the hydrogel enhanced. This was attributed to more Schiff base linkages and hydrogen bonds formed in the higher concentration of ADA. The elongation at break was about 23% regardless of the concentration of anthocyanin in the hydrogel when the CMC vs ADA was set to be 1:0.2. Enhancing the ratio of ADA to 0.3, the elongation at break decreased to 13% which demonstrated that the hydrogel became brittle.

Mechanical properties of the hydrogel were then characterized by a rheology test. Since ADA in the hydrogel has large effects on the mechanical properties, the concentration of ADA was studied. As shown in Fig. 3 (B), the storage modulus (G') and loss modulus (G'') of the hydrogels (hydrogel-1,2,3) between 0.1–100 rad/s were obtained. The storage modulus (G') was higher than the loss modulus (G'') which demonstrated that the hydrogel formed and was a solid. The storage modulus (G') was higher with higher concentration of ADA in the hydrogel at the same frequency which

demonstrated the mechanical properties became stronger. More Schiff base linkages and hydrogen bonds formed when more ADA was added, and thus, the mechanical properties were enhanced.

Fig. 3

3.4 Swelling property of the hydrogel

Due to the hydrophilic nature of biopolymers in the hydrogel, the hydrogel showed excellent swelling properties. The effects of concentration of ADA in the hydrogel was studied. As shown in Fig. 4 (A), the hydrogel-1 with low concentration of ADA shrunk at pH 3.0 and dissolved at pH 7.0 and 9.5. The hydrogel-2 and hydrogel-3 also shrunk at pH 3.0. The carboxyl group was in the form of -COOH at pH 3.0 which resulted in strong hydrogen bonds in the hydrogel network. The swelling ratio of hydrogel-3 was higher than the hydrogel-2 at pH 7.0 in that more carboxyl groups in the hydrogel would absorb more water. The swelling ratio of hydrogel-3 was slightly lower than the hydrogel-2 at pH 9.5. This may be because more ADA and deprotonation of the amino group together resulted in a compact hydrogel network at pH 9.5 which hindered the penetration of water.

The effects of anthocyanin concentration on the swelling ratio was also investigated. As shown in Fig. 4 (C), the hydrogel with various anthocyanin concentrations (hydrogel-4,2,5,6) shrunk at pH 3.0. The hydrogel-4, hydrogel-2 and hydrogel-5 with the same ADA concentration had a similar swelling ratio after 6 hours which demonstrated that the low concentration of anthocyanin had little effect on the swelling behavior. When the concentration of anthocyanin increased to 2.25 wt% (hydrogel-6), the swelling ratio was slightly lower than the hydrogel-4,2,5. This may be due to the high concentration of anthocyanin that resulted in a rigid network and thus reduced the adsorption

353 of water. As shown in Fig. 4 (D), hydrogel-4,2,5 cannot maintain a rectangular shape after swelling
354 for 6 hours whilst hydrogel-6 was still a rectangular hydrogel. Increasing the pH to 9.5 produced
355 almost the same swelling ratio in the hydrogel-4,2,5,6 demonstrating that the anthocyanin had little
356 effect on the swelling ratio of the hydrogels at pH 9.5. The deprotonation of amino group in CMC
357 induced generation of more hydrogen bonds. This made the hydrogel network more compact and
358 lowered the swelling ratio. As shown in Fig. 4 (D), the hydrogel can retain their rectangular shape
359 after swelling for 6 hours.
360
361 Fig. 4
362
363 **3.5 Gas responsive property of the hydrogel**
364 Anthocyanin is a pH sensitive dye which has been widely used as a pH indicator to detect the
365 freshness of meat. The color responsive properties of hydrogels containing anthocyanin were
366 evaluated. The CIELAB color space (*L*, *a*, *b* value) and digital images of the hydrogels under
367 ammonia or acetic acid gas were recorded. As shown in Fig. 5 (A), *a* value changed from -9.1 to 4.7
368 within 2 minutes under acetic acid gas which indicated that the color of the hydrogel changed from
369 greenish to reddish (S. Huang, Xiong, Zou, Dong, Ding, Liu, et al., 2019; X. Zhang, Chen, Dai, Cui,
370 & Lin, 2023). The digital images in Fig. 5 (D) shows that the color of the hydrogel changed from
371 green to red. The color change of the hydrogels under acetic acid gas was attributed to the color
372 change characteristics of anthocyanin. Further increase in the incubation time, caused a small
373 change in the *a* value and color of the hydrogel. This demonstrated that the hydrogel responded
374 quickly to the presence of acetic acid gas. The ΔE change of the hydrogel was also obtained. As

shown in Fig. 5 (A), the ΔE increased to 20 after 2 minutes exposure to the acetic acid gas which indicated that the color change can be observed by naked eye. Further increasing the incubation time, the ΔE change was less than 6 which indicated that the color change could hardly be observed by the naked eye. The ΔE change corresponded to the changes in the digital images of the hydrogels after incubation for different time intervals.

The color response of the hydrogel under ammonia gas was also obtained. As shown in Fig. 5 (B), *b* value and digital images of the hydrogel were recorded. *b* value changed from 7.0 to 24.0 indicating that the yellow color became deeper after exposure to ammonia gas. Further increasing the incubation time, the *b* value exhibited a small change which demonstrated that the active site in the dye had been saturated with ammonia gas. In addition, the color of hydrogels changed little which corresponding to the change in *b* value. The change in ΔE also corresponded to the changes in *b* value and digital images. ΔE increased to 17 after 2 minutes which demonstrated fast response to the ammonia gas and the color change can be observed by the naked eye.

Cyclic exposure of hydrogel to ammonia or acetic acid gas was also performed. The value of *a*, ΔE were measured and digital images obtained. As shown in Fig. 5 (D), the digital images showed that the color of the hydrogel changed from green to red after incubation in acetic acid gas for 2 minutes. The value of a changed from -8.1 to 5.3 and ΔE increased to 15 which indicated that the color change is obvious and can be observed by naked eye. The *a* and ΔE value changes corresponded to the color change of the hydrogel in the digital images. The hydrogel was then immediately put in the ammonia gas and incubated for 2 minutes. As shown in Fig. 5 (D), the color of hydrogel turned from red to green again. The value of *a* changed from 5.3 to -6.4 and ΔE changed from 15 to 6.6 which indicated that the color changed from reddish to greenish. The hydrogel was

then put in the acetic acid gas and incubated for 2 minutes. The color of hydrogel did not completely change from red to green. This may be because partial ammonia gas adsorbed on the hydrogel had been neutralized by the acetic acid gas. Subsequent placement in ammonia or acetic acid gas for 2 minutes, produced a small color change at the edge of the hydrogel. The value of *a* and change in ΔE were also small demonstrating that the color change cannot be observed by the naked eye.

Fig. 5

3.6 Freshness detection by the hydrogel sensors

Inspired by the color change of the hydrogel in gas immersion at different pHs, the hydrogel could be potentially used as indicator to detect the freshness of the meat. The hydrogel sensor was put in a box with chicken, fish or pork at 15°C. At different time intervals, the color change of the sensors and *b* value change were recorded. The hydrogel was firstly used as a sensor to detect the freshness of chicken. The pH changes of chicken and *b*, ΔE value change in the sensor were recorded. As shown in Fig. 6 (A), the pH of chicken is about 5.5 which demonstrated that the chicken is fresh (L. Lin, Mei, Shi, Li, Abdel-Samie, & Cui, 2023). After storing for 20 hours, the pH slightly increased to 5.7. The *b* value of the hydrogel sensor increased from -0.7 to 6.4 which suggested that the color turned light yellow. The *b* value change corresponded with the photographs of the hydrogel, as shown in Fig. 6 (B). The ΔE value change was 7 which was higher than 6.5, suggesting that the color change of the hydrogel sensor can be detected by the naked eye. Further increase in the storing time caused the chicken to spoil after 68 hours. The TVB-N of the chicken was 27.8 mg/100 mg and the pH was 6.7. The TVB-N and pH changes confirmed that the chicken spoiled. The *b* value

of the hydrogel increased to 15.2 which demonstrated that the yellow became deeper. The ΔE value increased to 16.3 and was higher than 13 which suggests that the color was totally different compared to its color at the beginning (Zhai, Sun, Cen, Wang, Zhang, Yang, et al., 2022). The hydrogel color changes suggest that it can potentially be used as an indicator to monitor the freshness of chicken.

The hydrogel can also be used as sensor to detect the freshness of fish and pork. As shown in Fig. 6 (C, D), the pH of the fish was 7.2 at the beginning indicating that the fish was fresh. After 20 hours storage, the pH slightly decreased to 7.0 and the *b* value of hydrogel increased to 8.9 which demonstrated that the color became yellow. The ΔE value changed to 8.7 compared with the original hydrogel. After storing for 44 hours, the pH of the fish decreased to 6.7 and TVB-N of the fish was 21.6 mg/100 mg which indicated that the fish spoiled (Zhai, et al., 2022). The decrease of pH may be attributed to the lactic acid produced by glycolysis and enzymatic reaction in fish. The ΔE value of the hydrogel increased to 14 after 44 hours demonstrating that the color change of the hydrogel can be easily observed by the naked eye. In addition, the hydrogel sensor can be used to detect the freshness of pork. As shown in Fig. 6 (E, F), the pH of the pork increased with storage time. The *b* and ΔE value of the hydrogel also enhanced after storing for different time intervals. After storing for 44 hours, the pH of the pork was 6.5 and the TVB-N was 15.7 mg/100 mg which demonstrated that the pork spoiled (J. Zhang, Zhang, Huang, Shi, Muhammad, Zhai, et al., 2023). The *b* and ΔE value changes were obvious and the color change of the hydrogel sensor can be detected by the naked eye. The hydrogel sensor showed excellent performance for monitoring the freshness of meat and can potentially be used as an indicator with promise in smart packaging.

Fig. 6

3.7 3D printing of the hydrogel

The hydrogel showed self-healing properties and can be potentially used as a bio-ink in 3D printing (Rajabi, McConnell, Cabral, & Ali, 2021). The 3D printing ability of the carboxymethyl chitosan hydrogel was preliminarily investigated. The hydrogels with ADA ratio of 0.2 and 0.3 were too viscous to be extruded from the needle. The hydrogel with CMC vs ADA as 1:0.1 was chosen as the inks. As shown in Fig. 7 (A), the hydrogel ink can be 3D printed on the white paper. The printed letter “I”, “C” and “G” on the paper surface was clear which demonstrated the printing quality was good. The hydrogel ink can also be printed on real food. The steamed bread was chosen as print substrate. As shown in Fig. 7 (B), the printed letter “H”, “O” and “C” on the steamed bread surface was clear. Further study may be performed to explore the detail 3D printing ability of the hydrogel ink. The self-healing carboxymethyl chitosan hydrogel can be potentially applied in 3D food printing.

Fig. 7

3.8 Degradation of the hydrogel

The self-healing carboxymethyl chitosan hydrogel with oxidized alginate showed biodegradable properties. The degradation is important for the hydrogel to be used as packaging materials. Herein, the biodegradation of hydrogel in soil, lake and simulated seawater was performed. The weight change and images of the hydrogels during the test were recorded. Note that

since higher ratio ADA resulted in a harder network, the hydrogels with different concentration of ADA (hydrogel-1,2,3) were chosen to study the biodegradable properties. As shown in Fig. 8 (A), the hydrogels (hydrogel-1,2,3) in the lakes quickly adsorbed the water and then degraded gradually. At day 2, though the weight of hydrogel-1 increased, the hydrogel-1 degraded into small pieces. Hydrogel-2 also started to degrade and became irregular in shape. Hydrogel-3 swelled and maintained a rectangular shape. This was because the hydrogel with less ADA possessed a weaker network. The hydrogel would easily break under the effects of microorganism and the chain repulsion force (Ding, Ren, Wang, Wu, Du, & Zou, 2021; H. Wang, Qian, & Ding, 2018). After degrading for 4 days in the lake, the hydrogel-1 totally degraded, whilst hydrogel-3 maintained its shape.

The degradation of the hydrogel in the simulated seawater was also studied. As shown in Fig. 8 (B), the degradation behaviors of the hydrogels were similar to the degradation in the lakes. However, the degradation was much slower than the degradation in the lakes because no microorganisms were presented in the simulated seawater and the salt in the solution inhibited the chain repulsion force. After 40 days, hydrogel-1 degraded into small pieces and hydrogel-2,3 maintained their shape. The results of degradation in the soil appear in Fig. 8 (C). Degradation behavior was similar to hydrogel in simulated seawater. The weight of hydrogel increased in the early stages due to gradual absorption of water. After 36 days, hydrogel-1 broke due to microorganism action. Whilst hydrogel-2 and 3 maintain rectangular shape, the weight gradually decreased. All in all, the hydrogels showed excellent degradable performance and had little effect on the environment. The hydrogels can be potentially used as disposable labels with great promise in smart packaging.

Fig. 8

4. Conclusions

In this study, we demonstrated that carboxymethyl chitosan hydrogels with anthocyanin can be prepared through crosslinking method with oxidized alginate. The oxidized alginate can crosslink with carboxymethyl chitosan through Schiff base linkages and hydrogen bonding. These dynamic bonds conferred self-healing properties to the hydrogels. The concentration of oxidized alginate had large effects on the physicochemical properties of the hydrogels. Higher content of oxidized alginate results in a more rigid network, enhancing the mechanical properties but weakening the self-healing of the hydrogels. The pH sensitive anthocyanin endowed the hydrogels with potential ability to detect the freshness of different meats of chicken, fish and pork. The hydrogels showed excellent degradable properties and can be decomposed in the lake, soil and simulated seawater. In addition, the self-healing hydrogel can be used as bio-ink applied in 3D printing. The biodegradable and acidic or basic gas responsive hydrogels can be potentially used as disposable labels applied in intelligent food packaging.

CRediT authorship contribution statement

Fuyuan Ding: Conceptualization, methodology, writing-original draft, funding acquisition, formal analysis, visualization. **Lin Fu**: Investigation, writing-original draft. **Xiaowei Huang**: Review & editing. **Jiyong Shi**: Review & editing. **Megan Povey**: Review & editing. **Xiaobo Zou**: Supervision, Review & editing.

Declaration of competing interest

The authors declared that they have no conflicts of interest to this work.

Data availability

Data will be made available on request.

Acknowledgements

This research has been supported by the China National Key R&D Program during the 14th Five-year Plan Period (Grant No. 2023YFE0105500). Project Funded by Youth Talent Cultivation Program of Jiangsu University and Jiangsu University for Senior Intellectuals (No. 20JDG18). Project Funded by Special Funds for Jiangsu Province Science and Technology Plans (BZ2024029).

References

Alnadari, F., Al-Dalali, S., Pan, F., Abdin, M., Frimpong, E. B., Dai, Z., AL-Dherasi, A., & Zeng, X. (2023). Physicochemical Characterization, Molecular Modeling, and Applications of Carboxymethyl Chitosan-Based Multifunctional Films Combined with Gum Arabic and Anthocyanins. *Food and Bioprocess Technology*, 1-19. https://doi.org/10.1007/s11947-023-03122-0.

Cao, S., Wang, S., Wang, Q., Lin, G., Niu, B., Guo, R., Yan, H., & Wang, H. (2023). Sodium alginate/chitosan-based intelligent bilayer film with antimicrobial activity for pork preservation and freshness monitoring. *Food Control, 148*, 109615. https://doi.org/10.1016/j.foodcont.2023.109615.

Chirani, N., Yahia, L., Gritsch, L., Motta, F. L., Chirani, S., & Farè, S. (2015). History and applications of hydrogels. *Journal of biomedical sciences, 4*(02), 1-23. https://doi.org/10.4172/2254-609X.100013.

Cui, H., Cheng, Q., Li, C., Khin, M. N., & Lin, L. (2023). Schiff base cross-linked dialdehyde β-cyclodextrin/gelatin-carrageenan active packaging film for the application of carvacrol on ready-to-eat foods. *Food Hydrocolloids, 141*, 108744. https://doi.org/10.1016/j.foodhyd.2023.108744.

Ding, F., Dong, Y., Wu, R., Fu, L., Tang, W., Zhang, R., Zheng, K., Wu, S., & Zou, X. (2022). An oxidized alginate linked tough conjoined-network hydrogel with self-healing and conductive

properties for strain sensing. *New Journal of Chemistry, 46*(24), 11676-11684. https://doi.org/10.1039/D2NJ02006H.

Ding, F., Hu, B., Lan, S., & Wang, H. (2020). Flexographic and screen printing of carboxymethyl chitosan based edible inks for food packaging applications. *Food Packaging and Shelf Life, 26*, 100559. https://doi.org/10.1016/j.fpsl.2020.100559.

Ding, F., Li, H., Du, Y., & Shi, X. (2018). Recent advances in chitosan-based self-healing materials. *Research on Chemical Intermediates, 44*, 4827-4840. https://doi.org/10.1007/s11164-018-3339-7.

Ding, F., Nie, Z., Deng, H., Xiao, L., Du, Y., & Shi, X. (2013). Antibacterial hydrogel coating by electrophoretic co-deposition of chitosan/alkynyl chitosan. *Carbohydrate polymers, 98*(2), 1547-1552. https://doi.org/10.1016/j.carbpol.2013.07.042.

Ding, F., Ren, P., Wang, G., Wu, S., Du, Y., & Zou, X. (2021). Hollow cellulose-carbon nanotubes composite beads with aligned porous structure for fast methylene blue adsorption. *International journal of biological macromolecules, 182*, 750-759. https://doi.org/10.1016/j.ijbiomac.2021.03.194.

Ding, F., Shi, X., Wu, S., Liu, X., Deng, H., Du, Y., & Li, H. (2017). Flexible polysaccharide hydrogel with pH-regulated recovery of self-healing and mechanical properties. *Macromolecular Materials and Engineering, 302*(11), 1700221. https://doi.org/10.1002/mame.201700221.

Ding, F., Wu, S., Wang, S., Xiong, Y., Li, Y., Li, B., Deng, H., Du, Y., Xiao, L., & Shi, X. (2015). A dynamic and self-crosslinked polysaccharide hydrogel with autonomous self-healing ability. *Soft Matter, 11*(20), 3971-3976. https://doi.org/10.1039/C5SM00587F.

Gopalakrishnan, K., & Mishra, P. (2023). Self-Healing Polymer a Dynamic Solution in Food Industry: a Comprehensive Review. *Food Biophysics*, 1-17. https://doi.org/10.1007/s11483-023-09780-z.

Guadagno, L., Vertuccio, L., Barra, G., Naddeo, C., Sorrentino, A., Lavorgna, M., Raimondo, M., & Calabrese, E. (2021). Eco-friendly polymer nanocomposites designed for self-healing applications. *Polymer, 223*, 123718. https://doi.org/10.1016/j.polymer.2021.123718.

Hu, B., Chen, L., Lan, S., Ren, P., Wu, S., Liu, X., Shi, X., Li, H., Du, Y., & Ding, F. (2018). Layer-by-layer assembly of polysaccharide films with self-healing and antifogging properties for food packaging applications. *ACS Applied Nano Materials, 1*(7), 3733-3740. https://doi.org/10.1021/acsanm.8b01009.

Huang, H.-L., Tsai, I.-L., Lin, C., Hang, Y.-H., Ho, Y.-C., Tsai, M.-L., & Mi, F.-L. (2023). Intelligent films of marine polysaccharides and purple cauliflower extract for food packaging and spoilage monitoring. *Carbohydrate polymers, 299*, 120133. https://doi.org/10.1016/j.carbpol.2022.120133.

Huang, K., & Wang, Y. (2022). Recent advances in self-healing materials for food packaging. *Packaging Technology and Science, 36*(3), 157-169. https://doi.org/10.1002/pts.2701.

Huang, S., Xiong, Y., Zou, Y., Dong, Q., Ding, F., Liu, X., & Li, H. (2019). A novel colorimetric indicator based on agar incorporated with Arnebia euchroma root extracts for monitoring fish freshness. *Food Hydrocolloids, 90*, 198-205. https://doi.org/10.1016/j.foodhyd.2018.12.009.

Lai, W.-F. (2023). Design and application of self-healable polymeric films and coatings for smart food packaging. *npj Science of Food, 7*(1). https://doi.org/10.1038/s41538-023-00185-3.

Lin, L., Mei, C., Shi, C., Li, C., Abdel-Samie, M. A., & Cui, H. (2023). Preparation and characterization

of gelatin active packaging film loaded with eugenol nanoparticles and its application in chicken preservation. *Food Bioscience, 53*, 102778. https://doi.org/10.1016/j.fbio.2023.102778.

Lin, Z., Bi, S., Du, G., Zhang, Y., Fu, H., Fu, L., Xu, C., & Lin, B. (2023). Self-Reinforced and Antibacterial Zn2+@ Vanillin/Carboxymethyl Chitosan Film for Food Packaging. *ACS Sustainable Chemistry & Engineering*. https://doi.org/10.1021/acssuschemeng.3c03109.

Lou, C., Tian, X., Deng, H., Wang, Y., & Jiang, X. (2020). Dialdehyde-β-cyclodextrin-crosslinked carboxymethyl chitosan hydrogel for drug release. *Carbohydrate polymers, 231*, 115678. https://doi.org/10.1016/j.carbpol.2019.115678.

Ma, L., Su, W., Ran, Y., Ma, X., Yi, Z., Chen, G., Chen, X., Deng, Z., Tong, Q., & Wang, X. (2020). Synthesis and characterization of injectable self-healing hydrogels based on oxidized alginate-hybrid-hydroxyapatite nanoparticles and carboxymethyl chitosan. *International journal of biological macromolecules, 165*, 1164-1174. https://doi.org/10.1016/j.ijbiomac.2020.10.004.

Muir, V. G., & Burdick, J. A. (2020). Chemically modified biopolymers for the formation of biomedical hydrogels. *Chemical reviews, 121*(18), 10908-10949. https://doi.org/10.1021/acs.chemrev.0c00923.

Patel, P., & Thareja, P. (2022). Hydrogels differentiated by length scales: A review of biopolymer-based hydrogel preparation methods, characterization techniques, and targeted applications. *European Polymer Journal, 163*, 110935. https://doi.org/10.1016/j.eurpolymj.2021.110935.

Rajabi, M., McConnell, M., Cabral, J., & Ali, M. A. (2021). Chitosan hydrogels in 3D printing for biomedical applications. *Carbohydrate polymers, 260*, 117768. https://doi.org/10.1016/j.carbpol.2021.117768.

Sai, F., Zhang, H., Qu, J., Wang, J., Zhu, X., Bai, Y., & Ye, P. (2022). Multifunctional waterborne polyurethane films: Amine-response, thermal-driven self-healing and recyclability. *Applied Surface Science, 573*, 151526. https://doi.org/10.1016/j.apsusc.2021.151526.

Santos, L. G., Alves-Silva, G. F., & Martins, V. G. (2022). Active-intelligent and biodegradable sodium alginate films loaded with Clitoria ternatea anthocyanin-rich extract to preserve and monitor food freshness. *International journal of biological macromolecules, 220*, 866-877. https://doi.org/10.1016/j.ijbiomac.2022.08.120.

Shen, Y., Wang, Z., Wang, Y., Meng, Z., & Zhao, Z. (2021). A self-healing carboxymethyl chitosan/oxidized carboxymethyl cellulose hydrogel with fluorescent bioprobes for glucose detection. *Carbohydrate polymers, 274*, 118642. https://doi.org/10.1016/j.carbpol.2021.118642.

Sultan, M., Hafez, O. M., & Saleh, M. A. (2022). Quality assessment of lemon (Citrus aurantifolia, swingle) coated with self-healed multilayer films based on chitosan/carboxymethyl cellulose under cold storage conditions. *International journal of biological macromolecules, 200*, 12-24. https://doi.org/10.1016/j.ijbiomac.2021.12.118.

Upadhyaya, L., Singh, J., Agarwal, V., & Tewari, R. P. (2013). Biomedical applications of carboxymethyl chitosans. *Carbohydrate polymers, 91*(1), 452-466. https://doi.org/10.1016/j.carbpol.2012.07.076.

Virk, M. S., Virk, M. A., Liang, Q., Sun, Y., Zhong, M., Tufail, T., Rashid, A., Qayum, A., Rehman, A., Ekumah, J. N., Wang, J., Zhao, Y., & Ren, X. (2024). Enhancing storage and gastroprotective

viability of *Lactiplantibacillus* plantarum encapsulated by sodium caseinate-inulin-soy protein isolates composites carried within carboxymethyl cellulose hydrogel. *Food Research International, 187*, 114432. https://doi.org/10.1016/j.foodres.2024.114432.

Wang, F., Xie, C., Tang, H., Hao, W., Wu, J., Sun, Y., Sun, J., Liu, Y., & Jiang, L. (2023). Development, characterization and application of intelligent/active packaging of chitosan/chitin nanofibers films containing eggplant anthocyanins. *Food Hydrocolloids, 139*, 108496. https://doi.org/10.1016/j.foodhyd.2023.108496.

Wang, H., Qian, J., & Ding, F. (2018). Emerging chitosan-based films for food packaging applications. *Journal of agricultural and food chemistry, 66*(2), 395-413. https://doi.org/10.1021/acs.jafc.7b04528.

Wang, J., Gao, Q., Zhao, F., & Ju, J. (2023). Repair mechanism and application of self-healing materials for food preservation. *Critical Reviews in Food Science and Nutrition*, 1-11. https://doi.org/10.1080/10408398.2023.2232877.

Xu, J., Liu, Y., & Hsu, S.-h. (2019). Hydrogels based on Schiff base linkages for biomedical applications. *Molecules, 24*(16), 3005. https://doi.org/10.3390/molecules24163005.

Yan, K., Ding, F., Bentley, W. E., Deng, H., Du, Y., Payne, G. F., & Shi, X.-W. (2013). Coding for hydrogel organization through signal guided self-assembly. *Soft Matter, 10*(3), 465-469. https://doi.org/10.1039/C3SM52405A.

Yin, H., Song, P., Chen, X., Huang, Q., & Huang, H. (2022). A self-healing hydrogel based on oxidized microcrystalline cellulose and carboxymethyl chitosan as wound dressing material. *International journal of biological macromolecules, 221*, 1606-1617. https://doi.org/10.1016/j.ijbiomac.2022.09.060.

Zhai, X., Sun, Y., Cen, S., Wang, X., Zhang, J., Yang, Z., Li, Y., Wang, X., Zhou, C., & Arslan, M. (2022). Anthocyanins-encapsulated 3D-printable bigels: A colorimetric and leaching-resistant volatile amines sensor for intelligent food packaging. *Food Hydrocolloids, 133*, 107989. https://doi.org/10.1016/j.foodhyd.2022.107989.

Zhang, J., Zhang, J., Huang, X., Shi, J., Muhammad, A., Zhai, X., Xiao, J., Li, Z., Povey, M., & Zou, X. (2023). Study on cinnamon essential oil release performance based on pH-triggered dynamic mechanism of active packaging for meat preservation. *Food Chemistry, 400*, 134030. https://doi.org/10.1016/j.foodchem.2022.134030.

Zhang, X., Chen, X., Dai, J., Cui, H., & Lin, L. (2023). A pH indicator film based on dragon fruit peel pectin/cassava starch and cyanidin/alizarin for monitoring the freshness of pork. *Food Packaging and Shelf Life, 40*, 101215. https://doi.org/10.1016/j.fpsl.2023.101215.

Zhang, X., Chen, X., Dai, J., Cui, H., & Lin, L. (2024). Edible films of pectin extracted from dragon fruit peel: Effects of boiling water treatment on pectin and film properties. *Food Hydrocolloids, 147*, 109324. https://doi.org/10.1016/j.foodhyd.2023.109324.

Zhao, L., Feng, Z., Lyu, Y., Yang, J., Lin, L., Bai, H., Li, Y., Feng, Y., & Chen, Y. (2023). Electroactive injectable hydrogel based on oxidized sodium alginate and carboxymethyl chitosan for wound healing. *International journal of biological macromolecules, 230*, 123231. https://doi.org/10.1016/j.ijbiomac.2023.123231.

Zhou, L., Chen, M., Guan, Y., & Zhang, Y. (2014). Multiple responsive hydrogel films based on dynamic Schiff base linkages. *Polymer Chemistry, 5*(24), 7081-7089. https://doi.org/10.1039/C4PY00868E.

Figure captions

Scheme 1 Schematic illustrating preparation and application of the self-healing carboxymethyl chitosan hydrogel.

Fig. 1. (A) Illustration of the preparation of carboxymethyl chitosan hydrogel containing anthocyanin through crosslinking with oxidized alginate; (B) FT-IR spectra of carboxymethyl chitosan, oxidized alginate, anthocyanin and the prepared hydrogel without anthocyanin (hydrogel-4) and with anthocyanin (hydrogel-2); (C) XRD pattern of carboxymethyl chitosan, oxidized alginate; (D) SEM images of the prepared hydrogel without anthocyanin (hydrogel-4) and with anthocyanin (hydrogel-2); (E, F) TG and DTG curves of carboxymethyl chitosan, the prepared hydrogel without anthocyanin (hydrogel-4) and with anthocyanin (hydrogel-2).

Fig. 2. Photographs demonstrating the preparation and the effects of concentration of oxidized alginate and anthocyanin on; (A) The self-healing properties of the carboxymethyl chitosan hydrogels; (B) schematic illustration of self-healing process of the carboxymethyl chitosan hydrogels; (C) Elastic responsive properties of self-healing hydrogel-2 characterized by rheometer; (D) Self-healing efficiency of the prepared hydrogels without anthocyanin (hydrogel-4) and with anthocyanin (hydrogel-2).

Fig. 3. (A) Mechanical properties of the hydrogels tested on a TA.XT2i texture analyser; (B) storage and loss modulus of hydrogel (hydrogel-1,2,3) characterized by oscillatory rheometry between 0.1–100 rad/s.

Fig. 4. (A, B) The effects of concentration of oxidized alginate on the swelling properties of the hydrogels (hydrogel-1,2,3); (C, D) The effects of concentration of anthocyanin on the swelling properties of the hydrogels (hydrogel-2,4,5,6).

Fig. 5. (A) The value of *a* and change in ΔE of hydrogel-2 in acetic acid gas under different time intervals; (B) the value of *b* and change in ΔE of hydrogel-2 in ammonia gas under different time intervals; (C) the value of *a* and change in ΔE of hydrogel-2 in repetitive ammonia and acetic acid gas immersions; (D) photographs of the hydrogel-2 in ammonia or acetic acid gas at various time intervals.

Fig. 6. (A) The ΔE, *b* value of the hydrogel and pH change of the chicken after storing at 15°C for different times; (B) the color response of the hydrogel-2 to the spoilage of chicken at different time intervals; (C) ΔE, *b* values of the hydrogel and pH change of the fish after storing at 15°C for different times; (D) the color response of the hydrogel-2 to the spoilage of fish; (E) ΔE, *b* values and pH change of the pork after storing at 15°C for different times; (F) color response of the hydrogel-2 to the spoilage of pork.

Fig. 7. (A) 3D printing of hydrogel-1 into letter “I C G” on white paper. (B) 3D printing of letters “H O C” in hydrogel-1 on steamed bread.

Fig. 8. The photographs and weight change over time for hydrogel-1,2,3 after decomposing (A) in the lake; (B) in simulated seawater and (C) soil.

Scheme 1

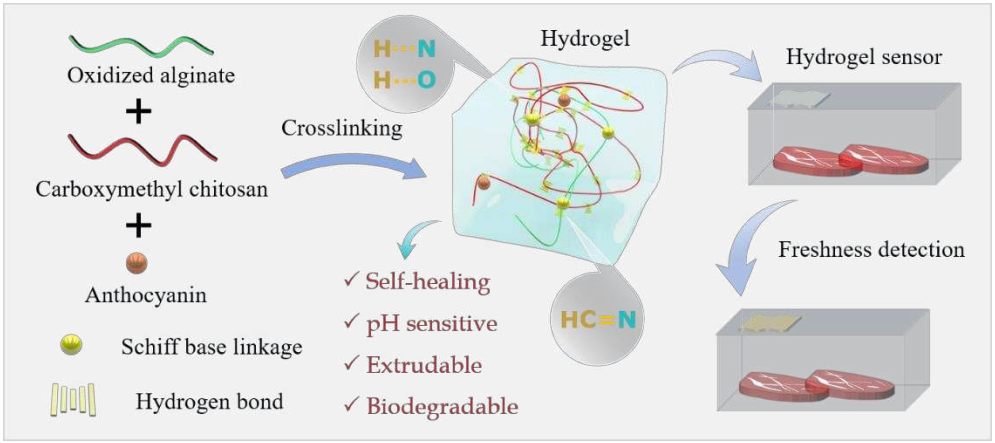

Fig. 1

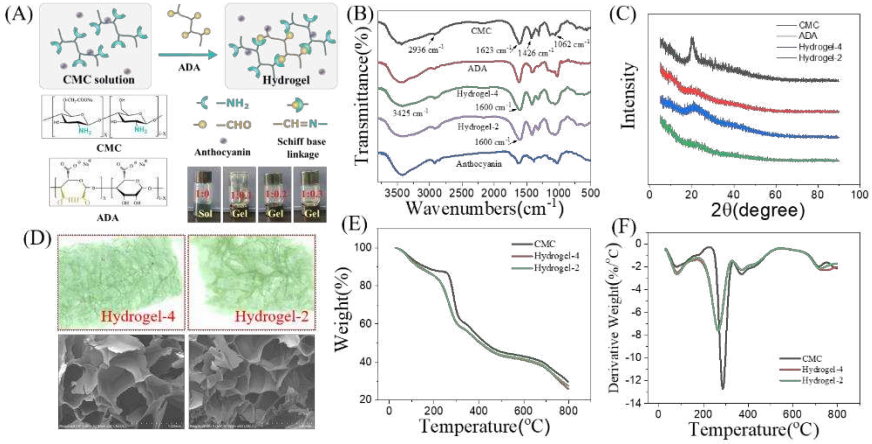

Fig. 2

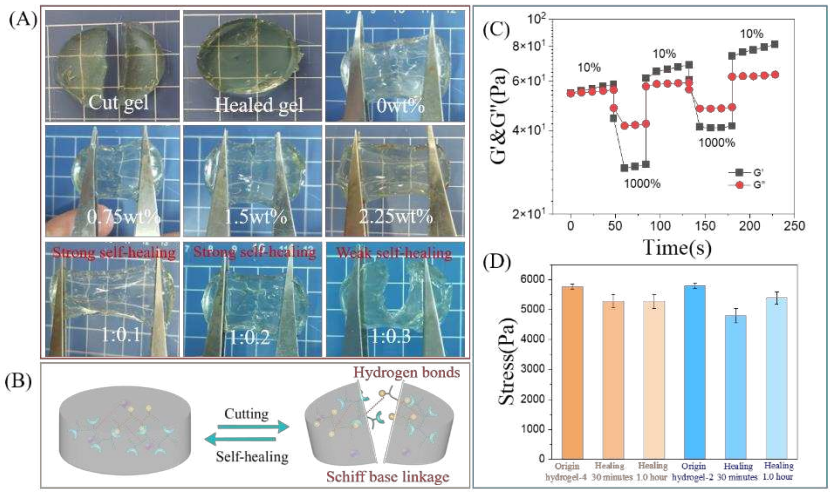

Fig. 3

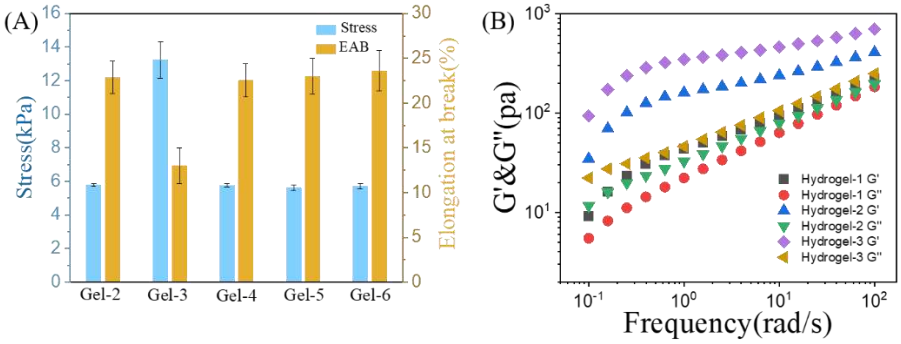
(A)
Stress
EAB
Stress(kPa)
Elongation at break(%)
Gel-2
Gel-3
Gel-4
Gel-5
Gel-6
(B)
G'&G''(pa)
Frequency(rad/s)
Hydrogel-1 G'
Hydrogel-1 G''
Hydrogel-2 G'
Hydrogel-2 G''
Hydrogel-3 G'
Hydrogel-3 G''

Fig. 4

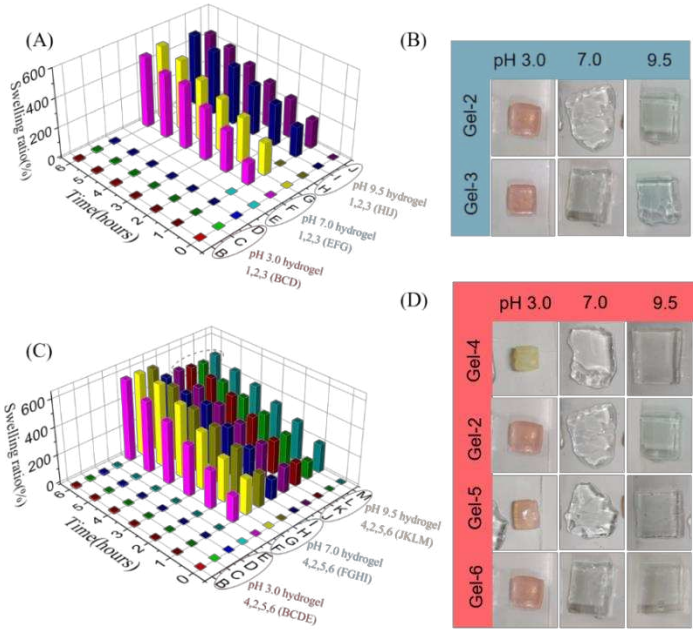
(A)
Swelling ratio(%)
Time(hours)
pH 9.5 hydrogel 1,2,3 (HIJ)
pH 7.0 hydrogel 1,2,3 (EFG)
pH 3.0 hydrogel 1,2,3 (BCD)
(B)
pH 3.0
7.0
9.5
Gel-2
Gel-3
(C)
Swelling ratio(%)
Time(hours)
pH 9.5 hydrogel 4,2,5,6 (JKLM)
pH 7.0 hydrogel 4,2,5,6 (FGHI)
pH 3.0 hydrogel 4,2,5,6 (BCDE)
(D)
pH 3.0
7.0
9.5
Gel-4
Gel-2
Gel-5
Gel-6

Fig. 5

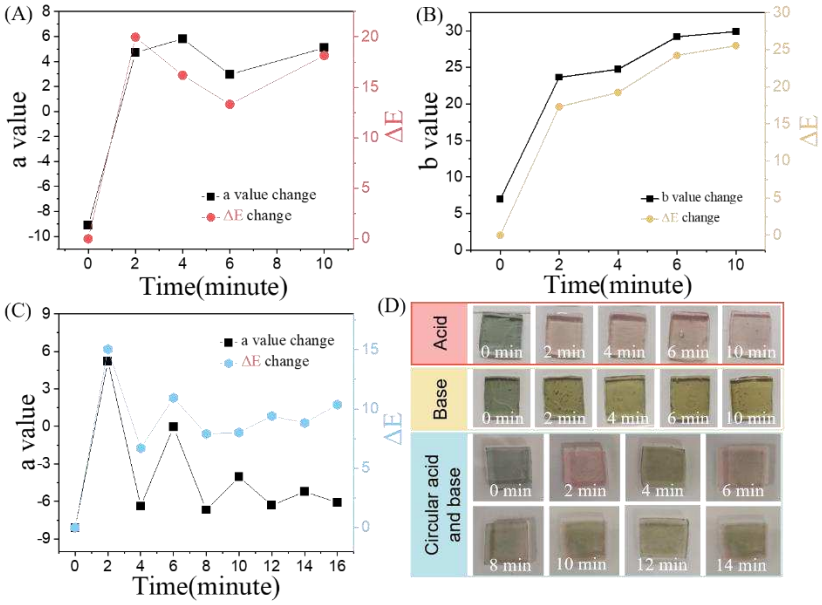

Fig. 6

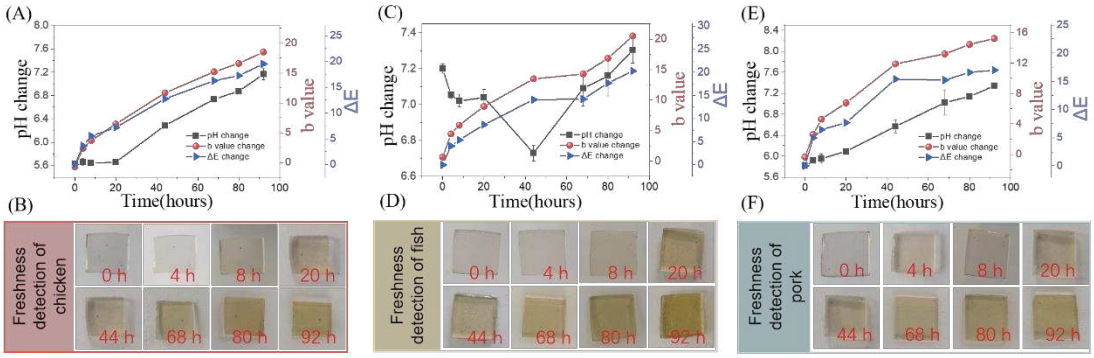

Fig. 7

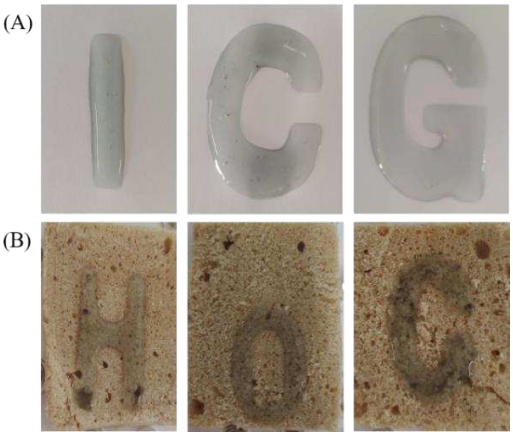

Fig. 8

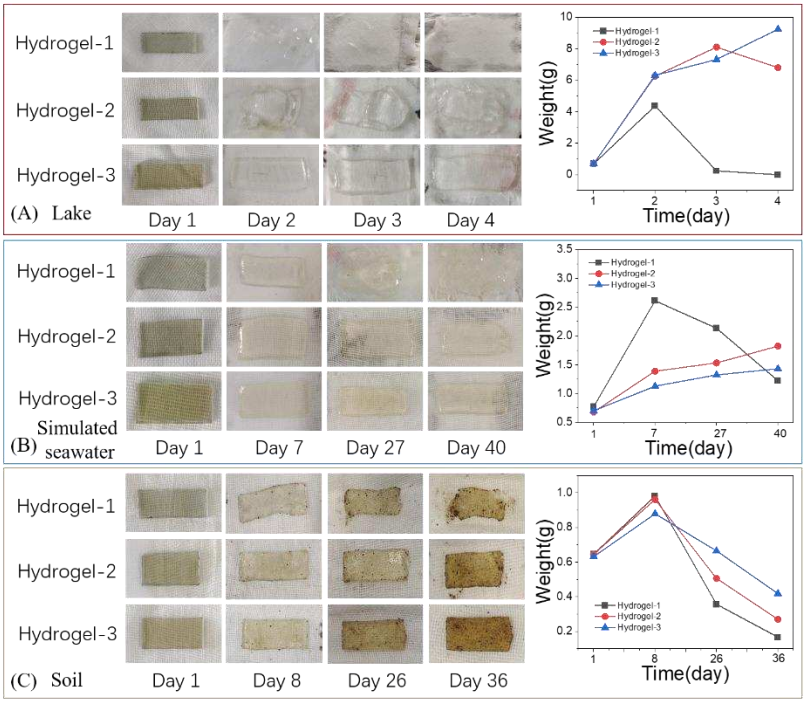
Hydrogel-1
Hydrogel-2
Hydrogel-3
(A) Lake
Day 1
Day 2
Day 3
Day 4
Weight(g)
Time(day)
Hydrogel-1
Hydrogel-2
Hydrogel-3
(B) Simulated seawater
Day 1
Day 7
Day 27
Day 40
Weight(g)
Time(day)
Hydrogel-1
Hydrogel-2
Hydrogel-3
(C) Soil
Day 1
Day 8
Day 26
Day 36
Weight(g)
Time(day)

Declaration of interests

☒ The authors declare that they have no known competing financial interests or personal relationships that could have appeared to influence the work reported in this paper.

☐The authors declare the following financial interests/personal relationships which may be considered as potential competing interests:

Fuyuan Ding
School of Food and Biological Engineering, International Joint Research Laboratory of Intelligent Agriculture and Agri-products Processing, Joint Laboratory of China-UK on Food Nondestructive Sensing, Jiangsu University, Zhenjiang, 212013, China

CRediT authorship contribution statement

Fuyuan Ding: Conceptualization, methodology, writing-original draft, funding acquisition, formal analysis, visualization. **Lin Fu**: Investigation, writing-original draft. **Xiaowei Huang**: Review & editing. **Jiyong Shi**: Review & editing. **Megan Povey**: Review & editing. **Xiaobo Zou**: Supervision, Review & editing.